J Nanopart Res (2015) 17:333
DOI 10.1007/s11051-015-3144-9

RESEARCH PAPER

Study of a shear thickening fluid: the dispersions of silica nanoparticles in 1-butyl-3-methylimidazolium tetrafluoroborate

Jianbin Qin · Guangcheng Zhang · Xuetao Shi · Min Tao

Received: 21 May 2015 / Accepted: 4 August 2015 / Published online: 13 August 2015

Abstract The dispersions was prepared by dispersing hydrophilic silica nanoparticles with an average diameter of 50 nm in 1-butyl-methylimidazolium tetrafluoroborate ([C_4mim][BF_4]), and investigated under the steady shear and oscillatory shear, respectively. Experimental results indicate that all of the dispersions present shear thinning, notable shear thickening, and shear thinning successively with increasing shear rate; the shear thickening behavior is derived from silica nanoparticle clusters and strongly controlled by silica nanoparticle content and temperature. The shear thickening fluid (STF) exhibits reversible property and transient response ability, and the time of transient response is no more than 100 ms. The conductivity of the STF is increased with increasing silica nanoparticle content, and the conductivity of 27 wt% dispersions is even two times as big as that of pure [C_4mim][BF_4]. The dispersions with high solid content dilate and present a phase transition changing from a liquid-like to a solid-like soft material in the shear thickening region. A theoretical model is developed to imitate the mechanism of shear thickening in the dispersions.

Keywords Dispersions · Shear thickening · Shear thinning · 1-butyl-methylimidazolium tetrafluoroborate · Silica nanoparticle · Clusters · Colloids

J. Qin (✉) · G. Zhang (✉) · X. Shi
Department of Applied Chemistry, School of Science, Northwestern Polytechnical University, 127#Youyi West Rd., Xi'an 710072, People's Republic of China
e-mail: fatedoomle@126.com

G. Zhang
e-mail: zhangguc@nwpu.edu.cn

M. Tao
Northwest Rubber Plastics Research & Design Institute Co., Xianyang 712000, People's Republic of China

Introduction

Ionic liquids (ILs) are composed entirely of ions and liquid with melting points near room temperature. ILs possess highly concentrated ionic atmosphere (Ueno et al. 2010a, b, c), negligible volatility, thermal stability, non-flammability, and high ionic conductivity (Ueno et al. 2010a, b, c). Therefore, ILs have attracted considerable interest in many fields of chemistry and in the chemical industry, used as solvents for synthesis and catalysis (Welton 1999), electrolytes (MacFarlane et al. 2010), lubricants and media for the formation and stabilization of nanoparticles (Ueno et al. 2008, 2009, 2010a, b, c; Wang et al. 2003).

Colloidal dispersions have been widely applied in many fields. The physical phenomena that present in colloidal dispersions, such as crystallization, glass-transition, and jamming transition, have attracted a great deal of attention (Trappe et al. 2001; Leunissen

et al. 2005). Two categories of soft materials consisting of colloidal particles have been reported (Stokes and Frith 2008). One is a colloidal gel, in which colloidal particles are unstable in the medium and form interconnecting three-dimensional networks, percolating through the entire space of the dispersion medium. The other is colloidal glass, which is formed in highly concentrated dispersions in which the colloidal particles are trapped within cages formed by the nearest neighbors.

Shear thickening fluid (STF) is a kind of dispersion whose rheological property takes place an abrupt change when encountering a strike. The apparent viscosity of STF changes so dramatically at a high-speed impact that STF may change from suspension to solid like. With the removal of impact, STF reverses its status to liquid like rapidly again. Thus, the shear thickening is a reversible non-Newtonian behavior. Some have seen thickening as a result of an order–disorder transition (Hoffman 1972, 1974, 1998). Other researchers have concluded that the reversible continue shear thickening (CST) in concentrated colloidal was due to the formation of a non-equilibrium and self-organized microstructure which was bound together by hydrodynamic forces, and denoted by the term clusters (Chow and Zukoski 1995; Bossis and Brady 1989; Foss and Brady 2000; Wagner and Brady 2009; Cheng et al. 2011; Heussinger 2013). For example, Xiang Cheng et al. (2011) have reported that hydroclusters were visualized when CST happened in concentrated colloidal with fast confocal microscopy. Recently, jamming and dilation for shear thickening in dense dispersions have been discussed (Lootens et al. 2005; Fall et al. 2008; Brown and Jaeger 2009; Nathan et al. 2013; Seto et al. 2013; Wyart and Cates 2014). The idea is that particles dilate, i.e., they want to expand when made to flow. This leads to an increase in normal stress and shear resistance. Dilation is a huge effect and may effectively jam the dispersion into a dynamically arrested state. Whether shear thickening in dispersions arises from order–disorder transitions or from formation of clusters induced by hydrodynamics lubrication remains controversial.

The most outstanding application of STF is used to exploit the soft protective composites, as reported in (Barnes 1989; Boersma et al. 1992; Bossis and Brady 1989; Brown and Jaeger 2009; Cates et al. 1998). Lee et al. (2003) researched the ballistic impact characteristics of Kevlar fabrics impregnated with STF. They found that the addition of STF to the fabric offers a significant enhancement in ballistic penetration resistance, without any loss in material flexibility. Wetzel et al. (2004) reported the effect of fluid viscosity, particle loadings, and particle size and shape on the behavior of STF-Kevlar composites. Decker et al. (2007) researched the stab resistance of STF-treated fabrics and found that the stab resistance exhibited significant improvements over neat fabric targets of equivalent areal density. Dramatic improvements in puncture resistance were observed under high- and low-speed loading conditions, while slight increases in cut protection were also observed. They proposed that the addition of STF primarily reduced the mobility of filaments and yarns in the impact zone. Kalman et al. (2007) reported that the polymer dispersion based STF-fabrics for protective applications. Srivastava et al. (2011) reported that the impact energy absorption performance of STF-Kevlar composite was enhanced at lower STF absorbing.

Most of the STF have been prepared and researched in low-molecular-weight polyethylene glycol, ethylene glycol, and other low-molecular-weight organic solvent. A number of dispersions containing ILs have been reported with respect to the dispersions of carbon nanotubes (Fukushima et al. 2003), crystalline polymers (Kawauchi et al. 2005), and silica nanoparticles (Ueno et al. 2008, 2009, 2010a, b, c; Ueno and Watanabe 2011; Wittmar et al. 2012; Novak and Britton 2013; Moosavi and Daneshvar 2014). The silica nanoparticle is the most common nanomaterial with a well-established surface chemistry, and its dispersions have been well explored in various media. However, a few researches have reported that certain colloidal dispersions of the silica nanoparticles in ILs presented shear thinning or shear thickening, such as $[C_4mim][BF_4]$, $[C_2mim][BF_4]$, and $[DEME][BF_4]$ (Ueno et al. 2009; Novak and Britton 2013; Moosavi and Daneshvar 2014). Only few studies have reported the shear thickening behaviors of these dispersions, let alone the mechanism of shear thickening. In this paper, we selected the dispersion of hydrophilic silica nanoparticles in $[C_4mim][BF_4]$ as a model system, and investigated the rheological and viscoelastic properties through steady shear and oscillatory shear, respectively. The mechanism of the shear thickening behavior about the dispersions was studied, and it was elaborated by a theoretical model.

Materials and methods

Materials

The silica nanoparticle with surface silanol groups was purchased from Aladdin Industrial Corporation, marked with an average diameter of 50 nm. The polyethylene glycol (Mw = 400) was purchased from Sinopharm Chemical Reagent Co., Ltd. Silica nanoparticles were dried under vacuum at 120 °C over 48 h before used. The 1-butyl-methylimidazolium tetrafluoroborate ([C_4mim][BF_4]) was provided by Lanzhou Institute of Chemical Physical, and was dried under vacuum at 80 °C over 48 h before used.

Preparation of the dispersions

All the dispersions were prepared by ultrasonication for no less than 2 h to ensure homogeneous mixing. The obtained samples were dried for 48 h under vacuum with heating at 80 °C prior to use for each measurement. The maximum solid content gotten in dispersions was 27 wt% for the surface effect of silica nanoparticles.

Measurements

Silica nanoparticle was characterized by field emission scanning electron microscopy (SEM, Quant FEG 450). Steady shear and oscillatory shear measurements were performed with a stress- and strain-controlled rheometer (Anton Paar Rheometer Physica MCR 301). The cone and plate system with a diameter of 50 mm, a cone angle of 2°, and a gap size of 0.99 mm was used. The measure point duration was 1 s for most of measurements, while it was 0.1 s for the transient response measurements. To eliminate any previous shear history and to allow the samples establish their equilibrium structures, a steady pre-shear was applied at a shear rate of 10 s^{-1} for 300 s followed by a 60-s rest period before each measurement. The conductivity of the dispersions with different silica nanoparticle content was performed with DDSJ-318 digital conductivity meter with Pt/Pt black electrodes (INESA instrument Co., Ltd) as quickly as the sample was taken out at room temperature.

Results and discussion

SEM image of silica nanoparticles is shown in Fig. 1. Silica nanoparticles present aggregation because surface silanol groups form hydrogen bonds.

Figure 2 shows the steady shear response of the dispersions in [C_4mim][BF_4] and PEG with different silica contents at 30 °C. At low shear rates, the viscosity of the dispersions slightly decreases, presenting the first shear thinning. Then, the viscosity begins to increase at a critical shear rate (γ_c), corresponding to a critical shear stress (τ_c), indicating that the onset of shearing thickening. A second shear thinning is observed in the end of shear application. In other words, all of the dispersions of hydrophilic silica nanoparticles in [C_4mim][BF_4] show shear thickening behavior in this work. With increasing silica nanoparticle content, as shown in Fig. 2a, the shear thickening behavior becomes more notable. The critical shear rate and critical shear stress, as shown in Fig. 2b, are important parameters of the shear thickening behavior. The critical shear rate decreases with increasing silica nanoparticle content, while the critical shear stress is constant on the whole in different concentration dispersions. Meanwhile, for the same concentration, the shear thickening behavior in the dispersions of [C_4mim][BF_4] is more noticeable than that in PEG as shown in Fig. 2a.

The viscosities of the hydrophilic silica nanoparticle dispersions in [C_4mim][BF_4] are relatively insensitive to the beginning shear rates. This suggests the absence of the silica network in dispersions. In other words, hydrophilic silica nanoparticles do not aggregate in dispersions with different solid contents. Repulsive force derived from steric hindrance or solvation force makes silica nanoparticles disperse in [C_4mim][BF_4], which has proposed by Ueno et al. (2009). The repulsive solvation force for ILs-silica system has been detected by surface force measurement and directly confirmed by atomic force microscopy (Liu et al. 2006; Atkin and Warr 2007). The shear thickening behavior is similar with hydrophilic silica dispersed in PEG (Mw = 400) as reported by Raghavan and Khan 1997. Compared with reports by Barnes (1989), Chow and Zukoski (1995), Lee and Wagner (2003), Cheng et al. (2011), and Heussinger (2013), we can make an ansatz that silica nanoparticles form clusters in the shear thickening region in [C_4mim][BF_4]. Silica nanoparticles may be ordered

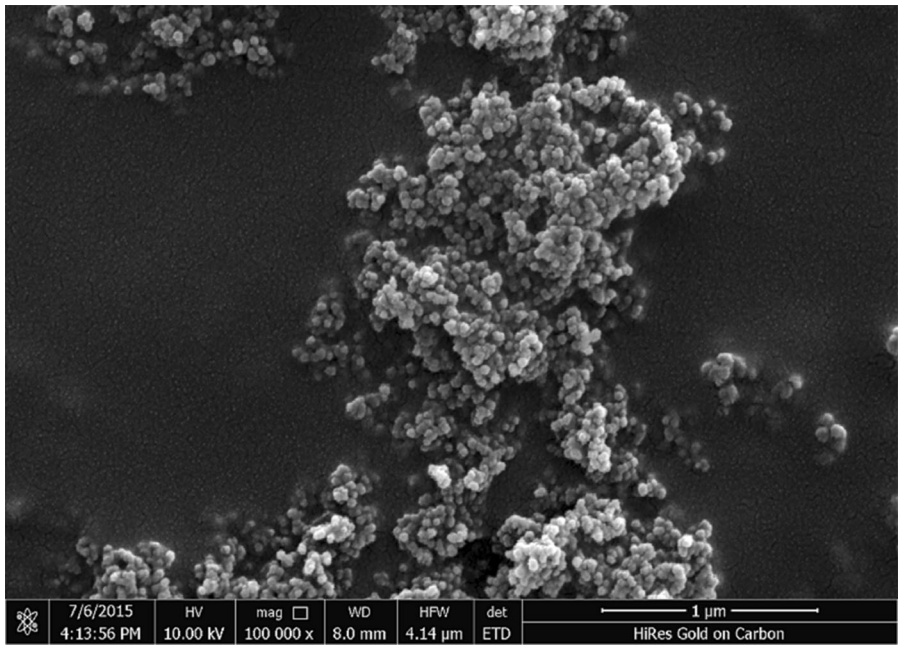

Fig. 1 SEM image of silica nanoparticles

under applied shear stress as reported by Chow and Zukoski (1995), Raghavan and Khan (1997), and Hoffman (1998). The ordered layers in the velocity–vorticity plane enable nanoparticles to flow without collision, thus reducing the viscosity. The long-range hydrodynamic force overcomes the short-range repulsive force between nanoparticles at the critical shear rate, and nanoparticles aggregate into clusters which lead to increased viscosity. The constant critical shear stress indicates that the interparticle repulsive forces are similar in dispersions with different silica concentrations. In high silica content dispersions, the average distance between nanoparticles is so small that it is easy for nanoparticles to move and form clusters, and therefore, the critical shear rate decreases. The number of nanoparticle clusters increases with increasing silica content or shear rate, which makes shear thickening behavior become more serious. In the 25 and 27 wt% dispersions, the nanoparticle clusters may be large and concentrated enough to aggregate and jam the dispersions in the gap between the plate and cone of the rheometer in the shear thickening region. This is similar with the jamming of cornstarch suspensions as reported by Lootens et al. (2005), Fall et al. (2008), Brown and Jaeger (2009), Heussinger (2013), and Nathan et al. 2013. However, the nanoparticle cluster is a metastable structure and it is destroyed easily at higher shear rates (Cates et al. 1998), which leads to a second shear thinning. The centrifugal force of the cone also contributes to the second shear thinning.

In addition, the existence of water may affect the rheology of dispersion because hygroscopic ILs easily adsorb water. However, it has demonstrated that water did not affect the characteristic rheological response in the dispersions of hydrophilic silica nanoparticles in $[C_4mim][BF_4]$ (Ueno et al. 2009).

Whether the clusters exist or not? We recorded the normal force of the cone in rheological measurements, as shown in Fig. 3, to study the shear thickening in detail. The upper cone of the rheometer will thus be attracted towards the bottom plate for negative values of the normal force and pushed away for positive values. The normal forces are negative values before shear thickening in all dispersions, and the absolute value of it will increase with increasing silica nanoparticle content. The negative normal forces may be attributed to strong hydrodynamic forces at low shear rates (Lootens et al. 2005). However, it is interesting that the positive normal force arises as soon as the shear thickening takes place except the 14 wt% dispersion. This indicates that the dispersions behave as dilatancy in the shear thickening region. However,

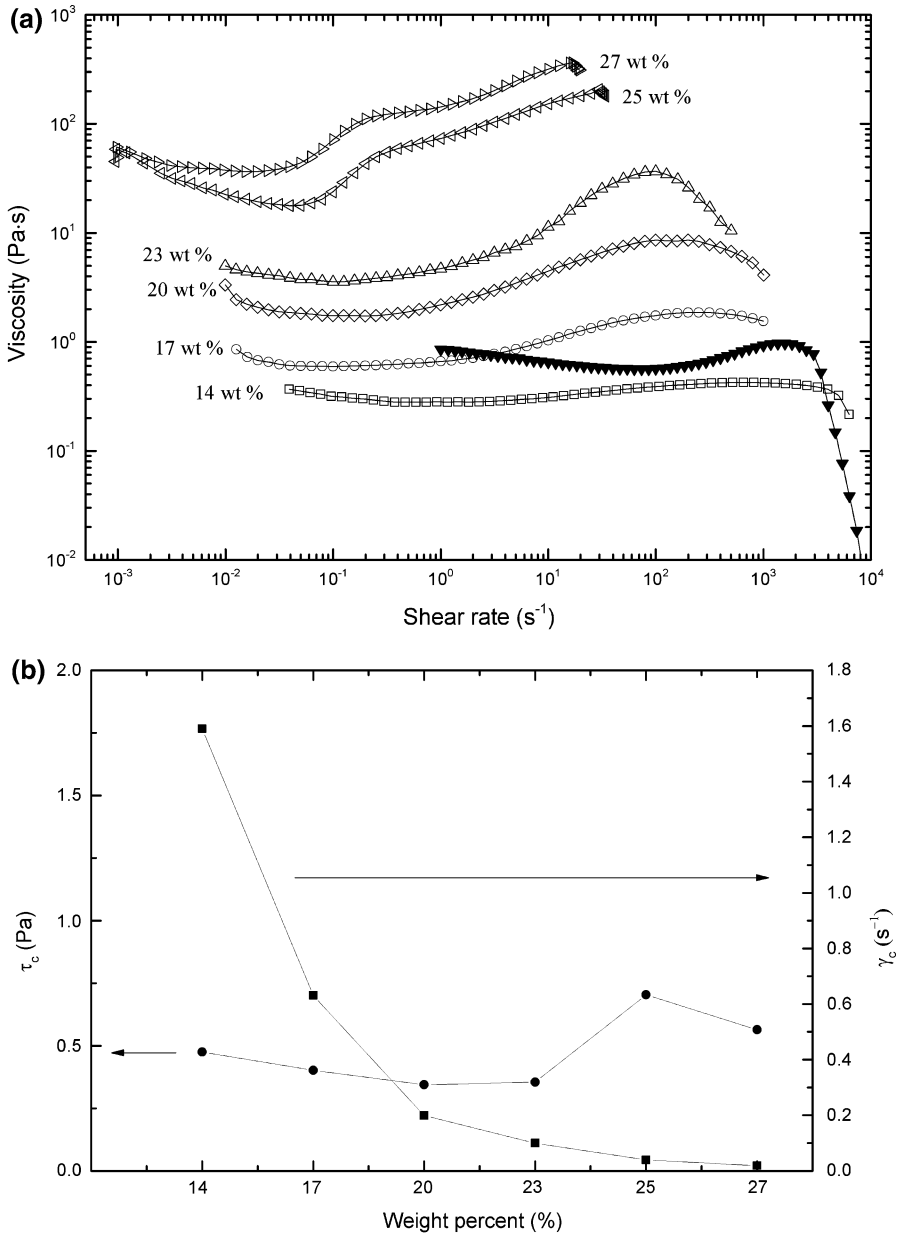

Fig. 2 **a** Shear rate (γ) dependencies of viscosity (η) for the dispersions in [C_4mim][BF_4] with different silica nanoparticle contents and in PEG400 with 23 wt% silica nanoparticles (*filled inverted triangle*); **b** the critical shear rate (γ_c) and critical shear stress (τ_c) versus silica nanoparticle wt%, respectively

both silica nanoparticle and [C_4mim][BF_4] cannot dilate. It is possible that silica nanoparticles aggregate and form clusters after a critical shear rate. Many clusters aggregate and jam the gap between the cone and the plate, resulting in the emergence of the positive normal forces. The quantity and volume of nanoparticle clusters will increase with increasing silica nanoparticle content or shear rate, so that the positive normal force increases. The divergent point of normal force lags that of viscosity, indicating that the nanoparticle clusters gradually grows with the increase of shear rate. In addition, the positive normal forces fluctuated at high shear rates also demonstrates the formation of clusters.

In order to further testify the clustering mechanism, we studied the influence of temperature on the shear thickening behavior of those dispersions. We know that the hydrogen bond is weakened with increasing temperature, which is not good for nanoparticles dispersing in media (Ueno et al. 2009, 2010a, b, c). On

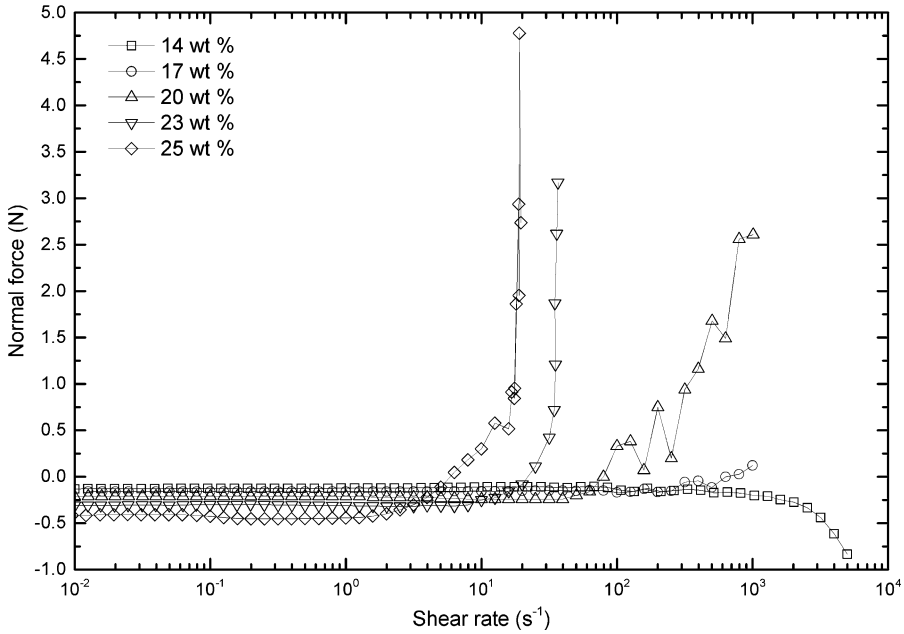

Fig. 3 Shear rate dependencies of normal force for the dispersions with different silica nanoparticle contents in [C_4mim][BF_4] under steady shear

the other hand, the thermal motion is enhanced with increasing temperature, which hinders the aggregation of nanoparticles. As shown in the inset of Fig. 4a, the viscosity of the pure [C_4mim][BF_4] is independent of shear rate, indicating that the [C_4mim][BF_4] is a Newtonian fluid in the measured range of shear rate. It will decrease as temperature increased, which agrees with Vogel–Fulcher–Tammann (VFT) equation (Moosavi and Daneshvar 2014). With increasing temperature, the critical shear rate increases and the shear thickening behavior recedes, as shown in Fig. 4a and b, which is according with the ansatz of clusters. In addition, the thermal motion of nanoparticles hinders the aggregation in dispersions, and therefore, the τ_c increases while the temperature changes from low (30 °C) to high (50 °C). However, the solvation force of silica nanoparticles will decrease at higher temperatures (Wakeham et al. 2009). So that the τ_c increases slightly at higher temperatures (70 and 100 °C).

The steady shear was performed in dispersions of silica nanoparticles in [C_4mim][BF_4] for both ascending and descending shear rate as shown in Fig. 5. After the point of the critical shear rate, the viscosity increases with increasing shear rate. As soon as the shear rate is decreased, the viscosity immediately declines. It is clear that the viscosities are in good agreement between shear rate ascending and descending. This can be concluded that the shear thickening behavior of the dispersions is reversible. The clusters maintained by lubrication force are metastable (Fernandez et al. 2013), and will be decomposed and dispersed in the media again as soon as the shear rate decreases with the decreased hydrodynamic force (Barnes 1989; Lee and Wagner 2003). The reversible property of the dispersions indicates that the dispersions are sensitive to shear rate. Figure 6 shows the thixotropic property of the dispersions with changing shear rates from 1 to 100 s^{-1} and then 1 s^{-1}. The viscosity keeps at about 2 Pa·s on the whole in the first region. And then the shear rate is increased to 100 s^{-1}, and the viscosity increases to 8.5 Pa·s instantaneously, no more than 100 ms. The shear rate is decreased for 1 s^{-1} again, and the viscosity decreases to about 2 Pa·s instantaneously again. The dispersions present transient response ability. This also indicates that the dispersions are very sensitive to shear rate, and can be explained by the instability of the nanoparticle clusters formed in the shear thickening region. Both the reversible property and the transient response ability suggest that the nanoparticle clusters are very sensitive to shear rate and transform dynamically. The nanoparticle clusters may become small at the initial phase of the high shear rate application, so that the viscosity decreases gradually as shown in Fig. 6.

We performed oscillatory shear measurements with a constant frequency (10 rad/s). Figure 7 shows the

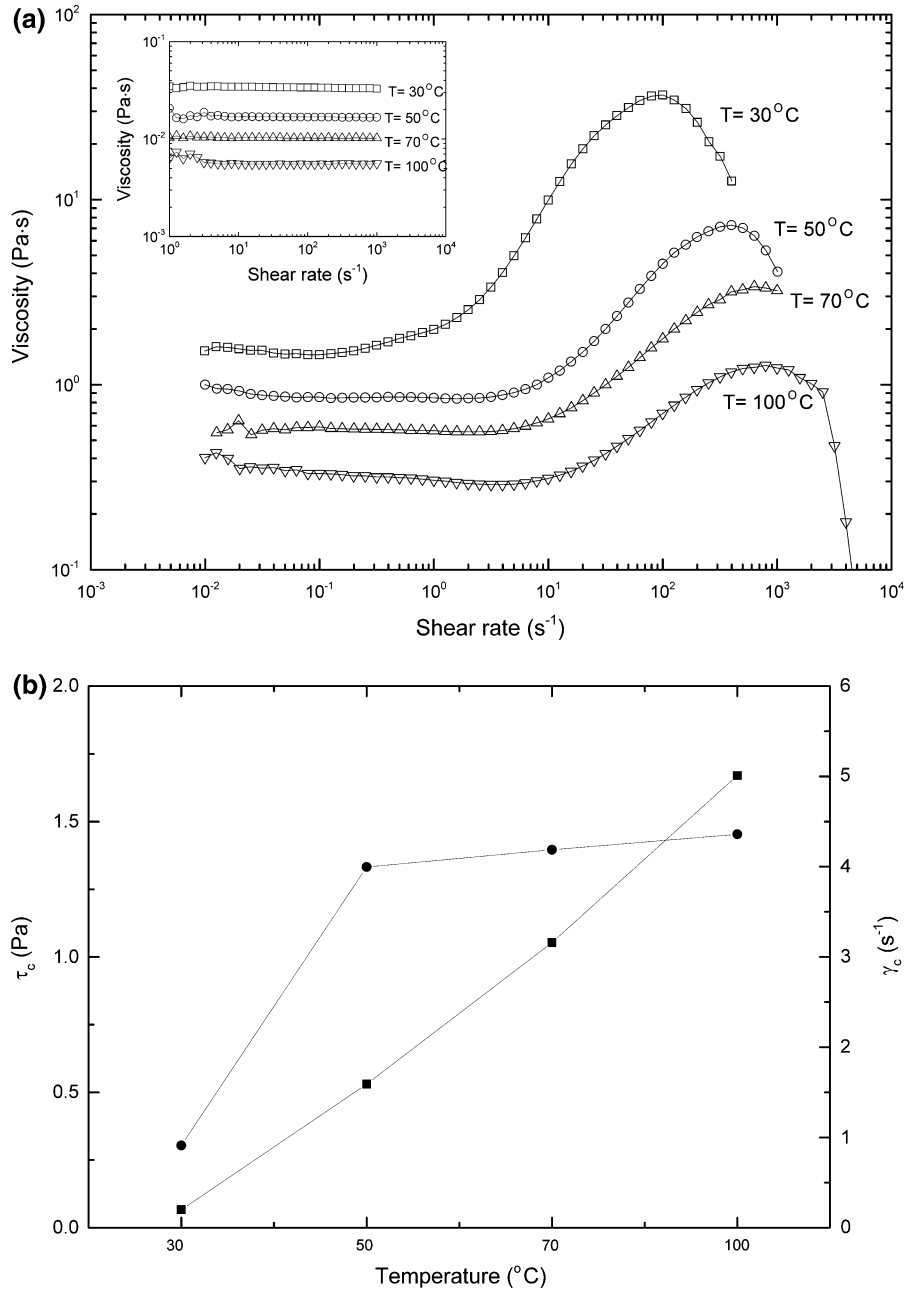

Fig. 4 Shear rate dependencies of viscosity for **a** the pure $[C_4mim][BF_4]$ and the 23 wt% dispersion at different temperatures, respectively; **b** the critical shear rate (γ_c) and critical shear stress (τ_c) versus temperature, respectively

loss modulus (G″), storage modulus (G′), complex viscosity ($|\eta^*|$), and normal force as a function of shear strain. All of dispersions present notable strain thickening, namely, shear thickening. The dispersions also behave as dilatancy in the strain thickening region. Whatever silica nanoparticle content, at low shear strain, the G′, G″, and $|\eta^*|$ behave as a slight strain thinning. Then, when a critical shear strain is reached, the G′, G″, and $|\eta^*|$ begin to increase at the same strain, namely strain thickening. The second strain thinning presents in the end of shear application. Furthermore, the G′, G″, $|\eta^*|$, and the peak value of positive normal forces are considerably enhanced with increasing silica nanoparticle content.

It is clear that the dispersion of silica nanoparticles in $[C_4mim][BF_4]$ is a dissipative system, as the G″ is

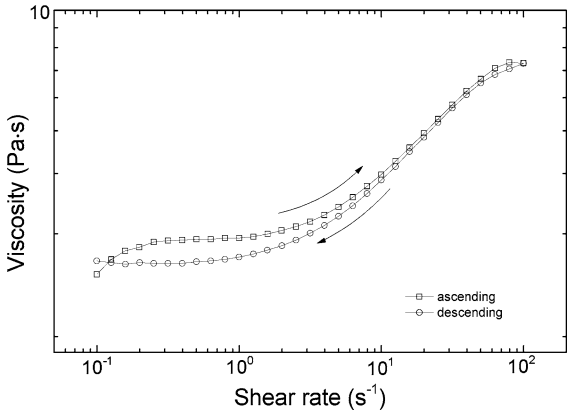

Fig. 5 Reversible shear thickening behavior of the dispersion composed of 20 wt% silica nanoparticles in [C_4mim][BF_4] at 30 °C

higher than G′ with a strong strain independency (Boersma et al. 1992). The loss modulus (G″) is higher than storage modulus (G′) at low shear strains, as shown in Fig. 7, also indicating that the dispersion is a non-flocculated system. The first shear thinning at low shear strains may be described by an increase of the anisotropy of the dispersions (Lootens et al. 2005). The G′ increased quickly after the critical shear strain implies that silica nanoparticles aggregate (Boersma et al. 1992). That is why the $|\eta^*|$ increases notably after the critical shear strain. In the meanwhile, the positive normal force arises because the nanoparticle aggregates penetrate the dispersions; the G″ is increased because the interparticle dissipation is enhanced for the aggregation of nanoparticles. These demonstrate that silica nanoparticles aggregate in the shear thickening region, nanoparticle aggregates will be destroyed at high shear strain, and the G′, G″, and $|\eta^*|$ behave as the second shear thinning. For low silica nanoparticle content dispersions, the number of silica nanoparticles aggregated in the shear thickening region is small, and the increase of G′, G″, and $|\eta^*|$ is little. In this case, the dimension of the nanoparticle cluster is smaller than that of the gap between the plate and cone, and the positive normal force does not turn up as shown in the inset of Fig. 7a. With increasing silica nanoparticle content, many nanoparticles aggregate in the shear thickening region, and the G′, G″, and $|\eta^*|$ greatly increase by 1–2 order of magnitudes. The peak value of normal forces increases as shown in the insets (Fig. 7b, c, d). In this case, the nanoparticle clusters are large and concentrated enough to jam the dispersions in the gap between the plate and cone, but do not organize in such a way that the dispersion becomes dilatant. It indicates that the dispersions change from a liquid-like to a solid-like soft material in the shear thickening region in high solid content ones. The G′ exceeds G″ in the shear thickening region for the dispersion with 27 wt% silica nanoparticles, also indicating that the dispersions are transformed into solid phase (Boersma et al. 1992). In addition, the

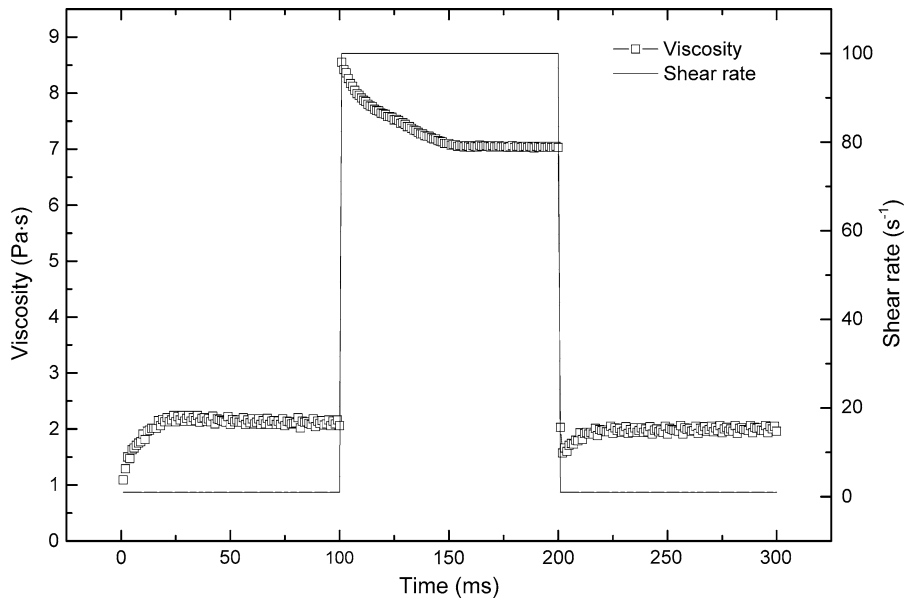

Fig. 6 Viscosity versus time for shear rate changed in the dispersion composed of 20 wt% silica nanoparticles in [C_4mim][BF_4] at 30 °C

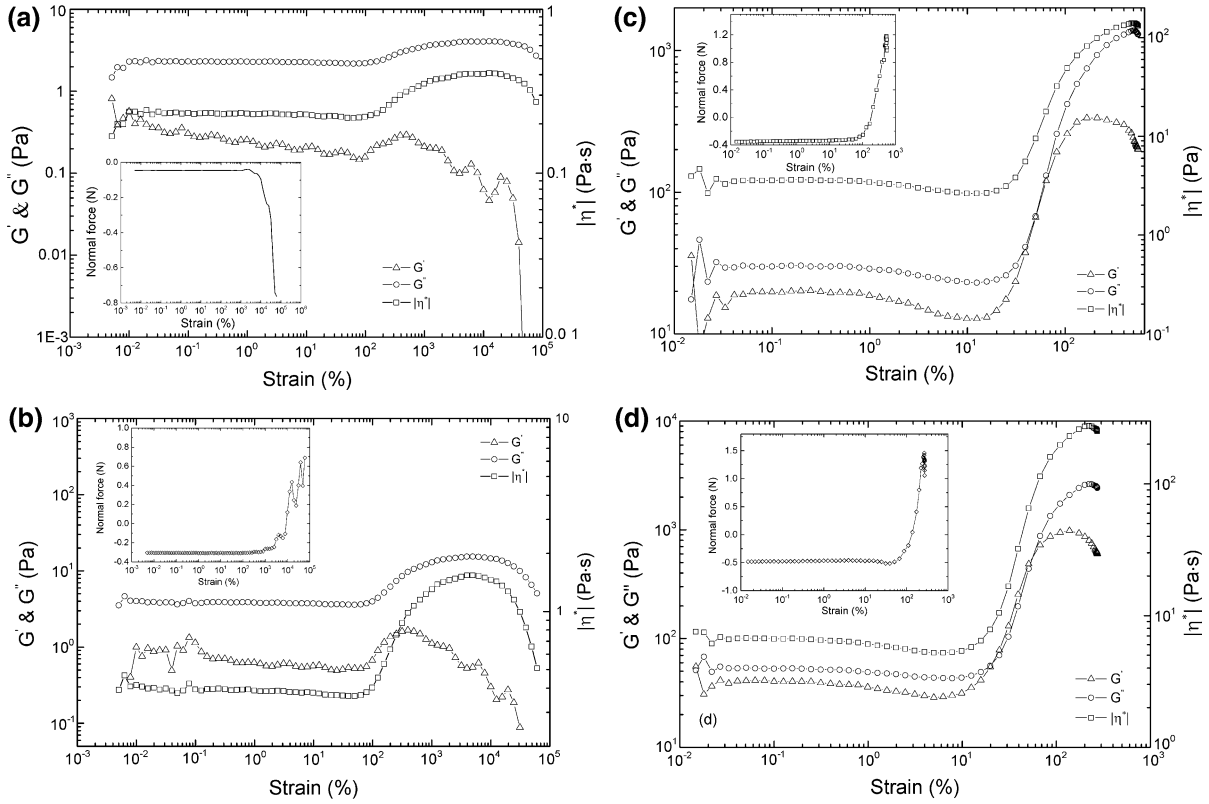

Fig. 7 Strain dependencies of complex viscosity ($|\eta^*|$), storage modulus (G′), and loss modulus (G″) for **a** 14 wt%, **b** 17 wt%, **c** 25 wt%, and **d** 27 wt% dispersions in [C_4mim][BF_4] at 30 °C with the frequency of 10 rad/s. *Insets* strain dependencies of normal force for different concentrated dispersions

shear stresses are in phase with an increase of normal forces as shown in Fig. 8, also implying that the dispersion is dilatant (Lootens et al. 2005). Comparing with steady shear, the nanoparticle aggregate can continuously adjust the constitution of itself under oscillatory shear. So that the peak value of normal force under oscillatory shear is weaker than that of under steady shear for the same solid content dispersions.

A theoretical model is developed, as shown in Fig. 9, to imitate the mechanism of shear thinning and shear thickening behavior about the dispersions of silica nanoparticles in [C_4mim][BF_4]. Silica nanoparticles are dispersed randomly in [C_4mim][BF_4] at the initial phase, as shown in Fig. 9a. Nanoparticles are ordered into layers in the velocity–vorticity plane at the onset of shear, which reduces the viscosity, presenting shear thinning as shown in Fig. 9b. Hydrodynamic force causes instability which breaks up the layered flow, and forces nanoparticles to aggregate at a critical shear rate. The nanoparticles form little clusters, resulting in the slight increase in low solid content dispersions as shown in Fig. 9c. Many bigger clusters are formed and even jam in the system in higher solid content dispersions, as shown in Fig. 9d, which makes the viscosity increase notably. The jammed nanoparticles will dilate under shear when they are confined as shown in Figs. 3, 7, and 8. Moreover, nanoparticle aggregation is a metastable structure, and partial section of it will be continually broken and rebuilt under shear, so that the normal force fluctuates, as shown in Figs. 3, 7, and 8.

Furthermore, the conductivity of the dispersions of silica nanoparticles in [C_4mim][BF_4] was studied as shown in Fig. 10. It is interesting that the conductivity of the dispersions is higher than that of the pure [C_4mim][BF_4] (Nishida et al. 2003), and it is enhanced with increasing silica nanoparticle content. The conductivity of 27 wt% dispersions is even two times as big as that of pure [C_4mim][BF_4]. That is to say, this STF possesses good conductivity. The solvation layer of the silica nanoparticles may contribute to the ionic

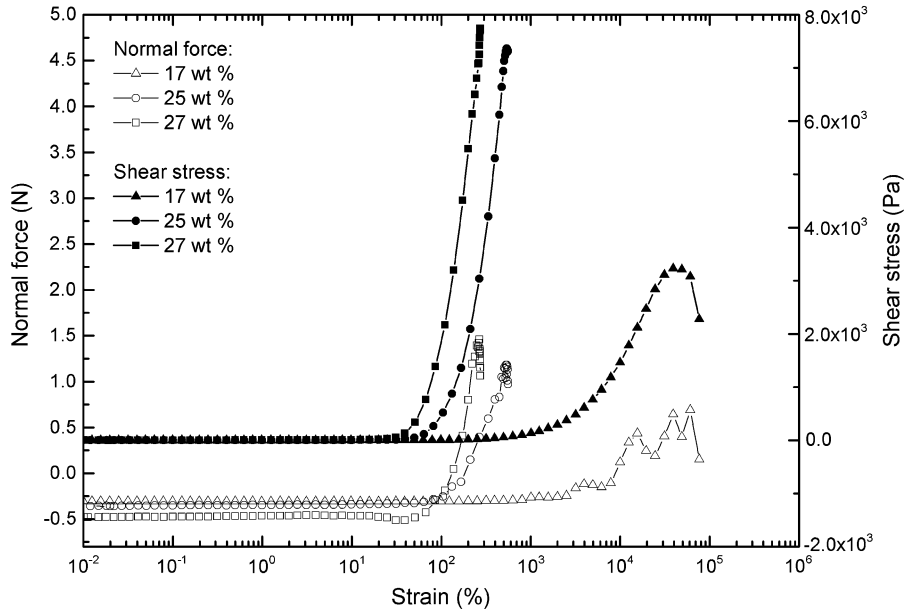

Fig. 8 Strain dependencies of normal force and shear stress for the dispersions in $[C_4mim][BF_4]$ with different silica nanoparticle concentrations at 30 °C with the frequency of 10 rad/s, respectively

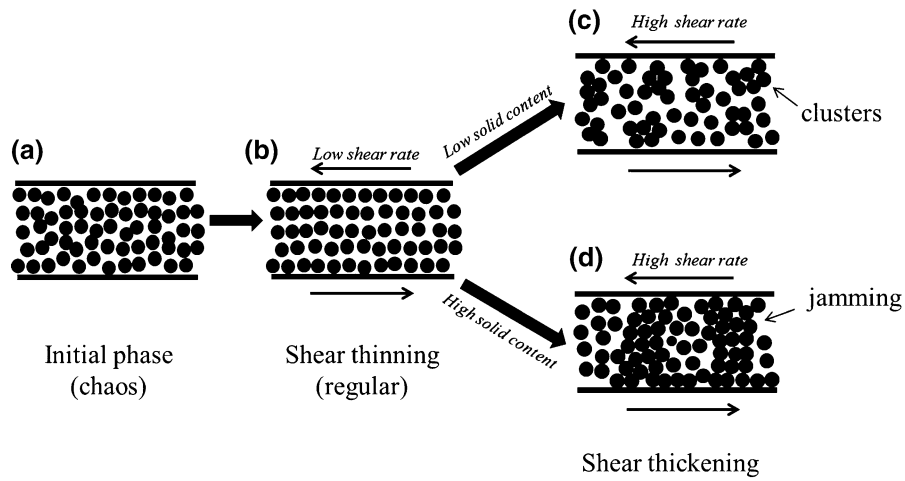

Fig. 9 Schematic illustrations of microstructure evolution under shearing for the dispersions of silica nanoparticles in $[C_4mim][BF_4]$

transport, which enhances the conductivity (Ueno et al. 2008). However, the hygroscopic may also enhance the conductivity of the $[C_4mim][BF_4]$. The nature of conductivity in the concentrated dispersions of hydrophilic silica nanoparticles in $[C_4mim][BF_4]$ needs further researches.

Conclusions

The dispersions of hydrophilic silica nanoparticles in $[C_4mim][BF_4]$ were systemically investigated. We find that the dispersions with different silica concentrations are non-flocculated and exhibit shear thinning, notable shear thickening, and shear thinning successively with increasing shear rate. At low shear rates, the regularly organized silica nanoparticles result in the first shear thinning. Above the critical shear rate, the notable shear thickening occurs due to the formation of the nanoparticle clusters or the jamming of nanoparticle clusters. The nanoparticle clusters are destroyed under strong shear stress, which leads to a second shear thinning. The shear thickening behavior of the STF becomes more significant with increasing

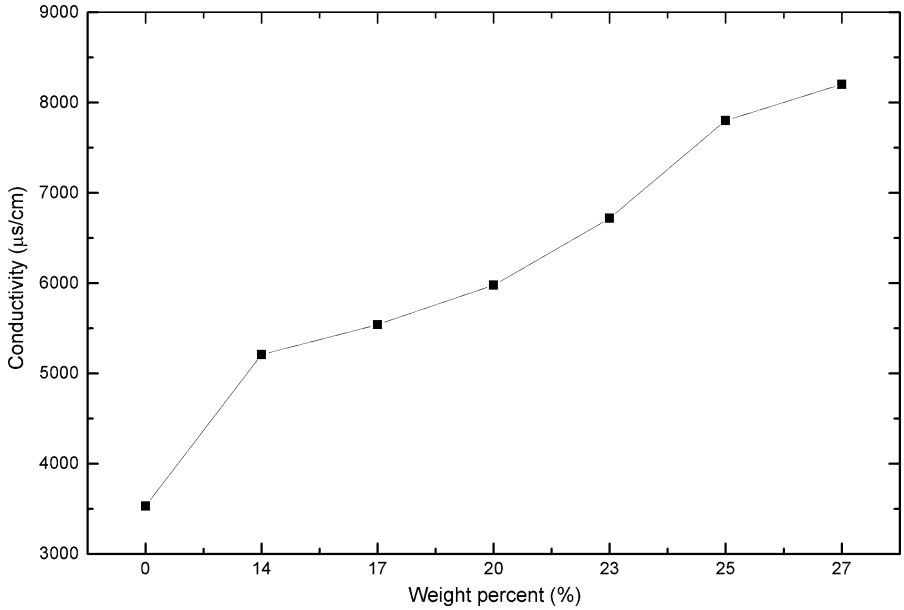

Fig. 10 Silica content dependencies of conductivity for the dispersions of silica nanoparticles in $[C_4mim][BF_4]$ at room temperature

silica nanoparticle content or with decreasing temperature. The critical shear rate increases with decreasing silica nanoparticle content or with increasing temperature. The critical shear stress of the STF is constant for different silica nanoparticle contents, while it is enhanced as temperature increased. The storage modulus, loss modulus, and complex viscosity of the STF are considerably enhanced with increasing silica nanoparticle content. The shear thickening ability of this STF is stronger than that of a conventional STF which based on low-molecular-weight polyethylene glycol (PEG400). Moreover, the STF of silica nanoparticles in $[C_4mim][BF_4]$ presents reversible property, transient response ability, and good conductivity. The time of transient response is no more than 100 ms and the conductivity of 27 wt% dispersions is even two times as big as that of pure $[C_4mim][BF_4]$. Meanwhile, the dispersions behave as phase transition in the shear thickening region, changing from a liquid-like to a solid-like soft material. The dilation of dispersions is observed in the shear thickening region under both steady shear and oscillatory shear. Moreover, the conductivity of the STF needs further researches. The STF has been used to exploit soft protective composites, as reported by Lee et al. (2003), Wetzel et al. (2004), Decker et al. (2007), and Srivastava et al. (2011). Compared with the STF prepared by polyethylene glycol (Mw = 200/400), the dispersions prepared by 1-butyl-methylimidazolium tetrafluoroborate, possessing more prominent shear thickening behavior, are the better candidate for exploiting protective composites. Moreover, they may be used to exploit functional material for their good conductivity.

Acknowledgments We gratefully acknowledge the Lanzhou Institute of Chemical Physical for providing the 1-butyl-3-methylimidazolium tetrafluoroborate ($[C_4mim][BF_4]$) used in this work.

Compliance with ethical standards

Conflict of Interest The authors declare no competing financial interest.

References

Atkin R, Warr GG (2007) Structure in confined room-temperature ionic liquids. J Phys Chem C 111(13):5162–5168. doi:10.1021/jp067420g

Barnes HA (1989) Shear-thickening ("dilatancy") in suspensions of nonaggregating solid particles dispersed in newtonian liquids. J Rheol (1978-present) 33(2):329–366. doi:10.1122/1.550017

Boersma WH, Laven J, Stein HN (1992) Viscoelastic properties of concentrated shear-thickening dispersions. J Colloid

Interface Sci 149(1):10–22. doi:10.1016/0021-9797(92)90385-Y

Bossis G, Brady JF (1989) The rheology of brownian suspensions. J Chem Phys 91:1866–1874. doi:10.1063/1.457091

Brown E, Jaeger HM (2009) Dynamic jamming point for shear thickening suspensions. Phys Rev Lett 103:086001. doi:10.1103/PhysRevLett.103.086001

Cates ME, Wittmer JP, Bouchaud JP, Claudin P (1998) Jamming, force chains, and fragile matter. Phys Rev Lett 81:1841–1844. doi:10.1103/PhysRevLett.81.1841

Cheng X, McCoy JH, Israelachvili JN, Cohen I (2011) Imaging the microscopic structure of shear thinning and thickening colloidal suspensions. Science 333:1276–1279. doi:10.1126/science.1207032

Chow MK, Zukoski CF (1995) Nonequilibrium behavior of dense suspensions of uniform particles: volume fraction and size dependence of rheology and microstructure. J Rheol 39:33–59. doi:10.1122/1.550687

Decker MJ, Halbach CJ, Nam CH, Wagner NJ, Wetzel ED (2007) Stab resistance of shear thickening fluid (STF)-treated fabrics. Compos Sci Technol 67(3):565–578. doi:10.1016/j.compscitech.2006.08.007

Fall A, Huang N, Bertrand F, Ovarlez G, Bonn D (2008) Shear thickening of cornstarch suspensions as a reentrant jamming transition. Phys Rev Lett 100:018301. doi:10.1103/PhysRevLett.100.018301

Fernandez N et al. (2013) Microscopic mechanism for shear thickening of non-brownian suspensions. Phys Rev Lett 111:108301. doi:10.1103/PhysRevLett.111.108301

Foss DR, Brady JF (2000) Structure, diffusion and rheology of brownian suspensions by stokes dynamics simulation. J Fluid Mech 407:167–200. doi:10.1017/S0022112099007557

Fukushima T, Kosaka A, Ishimura Y, Yamamoto T, Takigawa T, Ishii N, Aida T (2003) Molecular ordering of organic molten salts triggered by Single-walled carbon nanotubes. Science 300:2072–2074. doi:10.1126/science.1082289

Heussinger C (2013) Shear thickening in granular suspensions: interparticle friction and dynamically correlated clusters. Phys Rev E 88(050201(R)):1–4. doi:10.1103/PhysRevE.88.050201

Hoffman RL (1972) Discontinuous and dilatant viscosity behavior in concentrated suspensions. I. Observation of a flow instability. Trans Soc Rheol 16:155–173. doi:10.1122/1.549250

Hoffman RL (1974) Discontinuous and dilatant viscosity behavior in concentrated suspensions. II. Theory and experimental tests. J Colloid Interface Sci 46:491–506. doi:10.1016/0021-9797(74)90059-9

Hoffman RL (1998) Explanations for the cause of shear thickening in concentrated colloidal suspensions. J Rheol 42:111–123. doi:10.1122/1.550884

Kalman DP, Schein JB, Houghton JM, Laufer CN, Wetzel ED, Wagner NJ (2007) Polymer dispersion based shear thickening fluid-fabrics for protective applications. In: Proceedings of SAMPE, Baltimore, pp 3–7

Kawauchi T, Kumaki J, Okoshi K, Yashima E (2005) Stereocomplex formation of isotactic and syndiotactic poly(-methyl methacrylate) in ionic liquids leading to thermoreversible ion gels. Macromolecules 38:9155–9160. doi:10.1021/ma0517594

Lee YS, Wagner NJ (2003) Dynamic properties of shear thickening colloidal suspensions. Rheol Acta 42(3):199–208. doi:10.1007/s00397-002-0290-7

Lee YS, Wetzel ED, Wagner NJ (2003) The ballistic impact characteristics of Kevlar® woven fabrics impregnated with a colloidal shear thickening fluid. J Mater Sci 38(13):2825–2833. doi:10.1023/A:1024424200221

Leunissen ME, Christova CG et al (2005) Ionic colloidal crystals of oppositely charged particles. Nature 437:235–240. doi:10.1038/nature03946

Liu Y, Zhang Y, Wu G, Hu J (2006) Coexistence of liquid and solid phases of Bmim-PF_6 ionic liquid on mica surfaces at room temperature. J Am Chem Soc 128:7456–7457. doi:10.1021/ja062685u

Lootens D, van Damme H, Hémar Y, Hébraud P (2005) Dilatant flow of concentrated suspensions of rough particles. Phys Rev Lett 95:268302. doi:10.1103/PhysRevLett.95.268302

MacFarlane DR, Pringle JM, Howlett PC, Forsyth M (2010) Ionic liquids and reactions at the electrochemical interface. Phys Chem Chem Phys 12:1659–1669. doi:10.1039/B923053J

Moosavi M, Daneshvar A (2014) Investigation of the rheological properties of two imidazolium-based ionic liquids. J Mol Liq 190:59–67. doi:10.1016/j.molliq.2013.10.024

Nathan CC, Lauren BP et al (2013) Shear thickening of corn starch suspensions: does concentration matter? J Colloid Interface Sci 396:83–89. doi:10.1016/j.jcis.2013.01.024

Nishida T, Tashiro Y, Yamamoto M (2003) Physical and electrochemical properties of 1-alkyl-3-methylimidazolium tetrafluoroborate for electrolyte. J Fluor Chem 120:135–141. doi:10.1016/S0022-1139(02)00322-6

Novak J, Britton MM (2013) Magnetic resonance imaging of the rheology of ionic liquid colloidal suspensions. Soft Matter 9:2730–2737. doi:10.1039/C3SM27409H

Raghavan SR, Khan SA (1997) Shear-thickening response of fumed silica suspensions under steady and oscillatory shear. J Colloid Interface Sci 185:57–67. doi:10.1006/jcis.1996.4581

Seto R, Mari R, Morris JF, Denn MM (2013) Discontinuous shear thickening of frictional hard-sphere suspensions. Phys Rev Lett 111:218301. doi:10.1103/PhysRevLett.111.218301

Srivastava A, Majumdar A, Butola BS (2011) Improving the impact resistance performance of Kevlar fabrics using silica based shear thickening fluid. Mater Sci Eng, A 529:224–229. doi:10.1016/j.msea.2011.09.021

Stokes JR, Frith WJ (2008) Rheology of gelling and yielding soft matter systems. Soft Matter 4:1133–1140. doi:10.1039/B719677F

Trappe V, Prasad V, Cipelletti L, Segre PN, Weitz DA (2001) Similarities between protein folding and granular jamming. Nature 411:772–775. doi:10.1038/ncomms2177

Ueno K, Watanabe M (2011) From colloidal stability in ionic liquids to advanced soft materials using unique media. Langmuir 27:9105–9115. doi:10.1021/la103942f

Ueno K, Hata K, Katakabe T, Kondoh M, Watanabe M (2008) Nanocomposite Ion Gels based on silica nanoparticles and an ionic liquid: ionic transport, viscoelastic properties, and microstructure. J Phys Chem B 112:9013–9019. doi:10.1021/jp8029117

Ueno K, Imaizumi S, Hata K, Watanabe M (2009) Colloidal interaction in ionic liquids: effects of ionic structures and

surface chemistry on rheology of silica colloidal dispersions. Langmuir 25:825–831. doi:10.1021/la803124m

Ueno K, Sano Y, Inaba A, Kondoh M, Watanabe M (2010a) Soft glassy colloidal Arrays in an ionic liquid: colloidal glass transition, ionic transport, and structural color in relation to microstructure. J Phys Chem B 114:13095–13103. doi:10.1021/jp106872w

Ueno K, Tokuda H, Watanabe M (2010b) Ionicity in ionic liquids: correlation with ionic structure and physicochemical properties. Phys Chem Chem Phys 12:1649–1658. doi:10.1039/B921462N

Ueno K, Inaba A, Ueki T, Kondoh M, Watanabe M (2010c) Thermosensitive, soft glassy and structural colored colloidal array in ionic Liquid: colloidal glass to gel transition. Langmuir 26(23):18031–18038. doi:10.1021/la103716q

Wagner NJ, Brady JF (2009) Shear thickening in colloidal dispersions. Phys Today 10:27–32. doi:10.1063/1.3248476

Wakeham D, Hayes R, Warr GG, Atkin R (2009) Influence of temperature and molecular structure on ionic liquid solvation layers. J Phys Chem B 113(17):5961–5966. doi:10.1021/jp900815q

Wang P, Zakeeruddin SM, Comte P, Charvet R (2003) Enhance the performance of dye-sensitized solar cells by co-grafting amphiphilic sensitizer and hexadecylmalonic acid on TiO_2 nanocrystals. J Phys Chem B 107:14336–14341. doi:10.1021/jp0365965

Welton T (1999) Room-temperature ionic liquids: solvents for synthesis and catalysis. Chem Rev 99:2071–2084. doi:10.1021/cr980032t

Wetzel ED, Lee YS, Egres RG, Kirkwood KM, Kirkwood JE, Wagner NJ (2004) The effect of rheological parameters on the ballistic properties of shear thickening fluid (STF)–Kevlar composites. AIP Conf Proc 712:288. doi:10.1063/1.1766538

Wittmar A, Ruiz-Abad D, Ulbricht M (2012) Dispersions of silica nanoparticles in ionic liquids investigated with advanced rheology. J Nanopart Res 14:651. doi:10.1007/s11051-011-0651-1

Wyart M, Cates ME (2014) Discontinuous shear thickening without inertia in dense non-brownian suspensions. Phys Rev Lett 112:089302. doi:10.1103/PhysRevLett.112.098302